Atmospheric Environment 122 (2015) 171–182

Contents lists available at ScienceDirect

Atmospheric Environment

journal homepage: www.elsevier.com/locate/atmosenv

Evaluation of diesel fleet emissions and control policies from plume chasing measurements of on-road vehicles

Chui Fong Lau [a, b], Agata Rakowska [a], Thomas Townsend [a], Peter Brimblecombe [a], Tat Leung Chan [c], Yat Shing Yam [d], Griša Močnik [e, f], Zhi Ning [a, *]

[a] School of Energy and Environment, City University of Hong Kong, Tat Chee Avenue, Kowloon, Hong Kong
[b] Department of Applied Science, Hong Kong Institute of Vocational Education (Chai Wan), Hong Kong
[c] Department of Mechanical Engineering, The Hong Kong Polytechnic University, Hung Hom, Kowloon, Hong Kong
[d] Environmental Protection Department, The Government of the Hong Kong Special Administrative Region, Hong Kong
[e] Aerosol d.o.o., Ljubljana, Slovenia
[f] Jožef Stefan Institute, Ljubljana, Slovenia

HIGHLIGHTS

- Gini coefficient was used to quantify the inequality of emission within fleets.
- Multi-pollutant control strategy needs to control vehicle emissions.
- There exist high emitters even in newer vehicle fleets.
- Identification and removal of high emitters is a cost-effective emission control.

ARTICLE INFO

Article history:
Received 6 April 2015
Received in revised form
15 September 2015
Accepted 17 September 2015
Available online 21 September 2015

Keywords:
Secondary NO_2
Particle emissions
Black carbon
High-emitters
Euro emission standards
Heavy duty diesel vehicles

ABSTRACT

Vehicle emissions are an important source of urban air pollution. Diesel fuelled vehicles, although constituting a relatively small fraction of fleet population in many cities, are significant contributors to the emission inventory due to their often long mileage for goods and public transport. Recent classification of diesel exhaust as carcinogenic by the World Health Organization also raises attention to more stringent control of diesel emissions to protect public health. Although various mandatory and voluntary based emission control measures have been implemented in Hong Kong, there have been few investigations to evaluate if the fleet emission characteristics have met desired emission reduction objectives and if adoption of an Inspection/Maintenance (I/M) programme has been effective in achieving these objectives. The limitations are partially due to the lack of cost-effective approaches for the large scale characterisation of fleet based emissions to assess the effectiveness of control measures and policy. This study has used a plume chasing method to collect a large amount of on-road vehicle emission data of Hong Kong highways and a detailed analysis was carried out to provide a quantitative evaluation of the emission characteristics in terms of the role of high and super-emitters in total emission reduction, impact of after-treatment on the multi-pollutants reduction strategy and the trend of NO_2 emissions with newer emission standards. The study revealed that not all the high-emitters are from those vehicles of older Euro emission standards. Meanwhile, there is clear evidence that high-emitters for one pollutant may not be a high-emitter for another pollutant. Multi-pollutant control strategy needs to be considered in the enactment of the emission control policy which requires more comprehensive retrofitting technological solutions and matching I/M programme to ensure the proper maintenance of fleets. The plume chasing approach used in this study also shows to be a useful approach for assessing city wide vehicle emission characteristics.

1. Introduction

On-road vehicle emission is one of the major sources of air pollution in the atmosphere, especially in urban areas. Diesel

* Corresponding author.
E-mail address: zhining@cityu.edu.hk (Z. Ning).

http://dx.doi.org/10.1016/j.atmosenv.2015.09.048
1352-2310/

fuelled vehicles of different fleets dominate in European countries (Schipper et al., 2002), while they constitute only a smaller fraction of total fleet in other areas serving mostly for goods and public transport due to their higher power rate compared with other fuelled vehicles. However, they have a disproportionally major contribution in the inventory because of their longer mileage of operation and significantly higher particulate matter (PM) emissions than vehicles using other fuels (Gertler, 2005). Furthermore, the International Agency for Research on Cancer recently classified diesel engine exhaust as a Group I carcinogen based on its association with lung cancer (Attfield et al., 2012; Silverman et al., 2012), which raises significant concerns for the public health of urban populations who tend to have frequent exposure to air pollutants from diesel exhaust. Hong Kong is a large and densely populated city, which experiences high levels of air pollution both in terms of pollutants generated on roads and that transported from the increasingly industrialised Pearl River Delta (Hagler et al., 2006; Louie et al., 2005). In 2016, tighter air quality objectives will come into force that will bring the city in line with WHO guidelines. Nevertheless the exposure patterns of Hong Kong residents, who largely live in crowded urban areas and take public transport along crowded city streets are exposed to particular combinations of pollutants that originate from traffic (Yang et al., 2015).

The government of the Hong Kong Special Administrative Region is aware of the importance of roadway vehicles as a source and has, over the years, introduced a range of regulations to reduce vehicle emissions, especially targeting diesel vehicles, as shown in Table S1. After these mandatory and voluntary based emission control measures have been successfully implemented (HKEPD, 2011, 2013), the Hong Kong Environmental Protection Department (HKEPD) has been assessing the effectiveness of the measures from the air quality data gathered by its monitoring network. However, there have been few investigations targeting their effects on on-road fleet emissions. A few studies have also pointed out the importance of proper vehicle maintenance in the effective operation of emission control devices (Edesess, 2011; Ning et al., 2012), but there has been little evidence of how Inspection/Maintenance (I/M) implementation affects aggregate fleet emissions.

The limitations are partially due to the lack of cost-effective approaches for the large scale characterisation of fleet-based emissions to assess the effectiveness of control measures and policy. For example, the chassis dynamometer method can provide comprehensive emission characteristics of individual vehicles in laboratory operation conditions (Pakbin et al., 2009), but is unable to cost-effectively test a large number of vehicles to represent the variation of emissions among the vehicle fleet (Franco et al., 2013). Portable Emissions Measurement System (PEMS) has the advantage of simulating real-world driving conditions and providing high resolution emission data (Rubino et al., 2010; Weiss et al., 2012), but the long turnover time of vehicle tests limits its application for large scale vehicle tests (Franco et al., 2013). A remote sensing system using infrared and ultraviolet absorption has proved efficient in capturing a large number of emission data in a short time (Chan et al., 2004; Ning and Chan, 2007), but there is still limitation in its application in measuring PM emission from diesel fuelled vehicles (Moosmüller et al., 2003). Recently, we have adopted a new plume chasing approach and sampled a range of vehicle fleets in Hong Kong to investigate the inter- and intra-fleet emission characteristics (Ning et al., 2012).

The current study presents a more comprehensive plume chasing campaign in Hong Kong targeting on-road diesel vehicles and also links the emissions of individual vehicles with the corresponding registration information. The principal objectives of the study are to develop a quantitative understanding of the fleet emissions issues and to elucidate the effectiveness of local emission control measures and policy. The fleet based PM and gas emission factors are presented with a quantitative measure of Gini coefficient introduced to compare the distribution of BC and NO_x emission factors and to identify the role of high-emitters in contributing to total emissions. We also investigate the degree of overlapping of high-emitters for different pollutant emissions to evaluate the effectiveness of retrofitting for emission control. Lastly, we evaluate the role of ozone in secondary NO_2 formation inside plume and present real-world ratios of primary NO_2 and NO_x from the measured heavy duty diesel.

2. Experimental methodology

2.1. Mobile platform setup

The plume chasing measurements were performed using the On-road Plume Chasing and Analysis System (OPCAS), that has been developed by our group for high time resolution on-road air quality and plume measurements. OPCAS comprises three major components: power supply module, sample analysis module, and data acquisition and processing module. Schematic diagram of OPCAS was depicted in supplementary data of the previous studies (Ning et al., 2012). It is powered by an Uninterrupted Power Supply capable for about 5-h operation. The sample analysis module was set up with separate sampling lines – one for gaseous pollutants which include CO_2, NO/NO_2 and O_3 and the other for particulate pollutants which include $PM_{2.5}$ mass, ultrafine particle (UFP) number, and black carbon (BC). Teflon tubing and fittings were used for the gas line while conductive tubing and stainless steel fittings were used for PM measurements. The details of all the measuring devices are listed in Table 1. In this study, the OPCAS was configured with an inlet installed in the front of a mobile platform towards the direction of driving to capture the plume of the target vehicle. Black carbon was measured with an Aethalometer (Model AE33, Magee Scientific) which features a parallel light absorption measurement on two sampling channels (from the same inlet stream) with different rates of aerosol accumulation to compensate filter loading effect (Drinovec et al., 2015). $PM_{2.5}$ mass concentration was measured by DustTrak II with $PM_{2.5}$ inlet connected inline and the concentrations were presented without a correction factor. The data presented in this study serves only as a reference for intercomparison among different fleets and not intended to compare with gravimetric PM emission standards. Isokinetic sampling was not considered here because particulate pollutants emitted from vehicles are of submicron size range (Morawska et al., 2007; Ning et al., 2013), with insignificant isokinetic sample error (Baron and Willeke, 2001). The ozone concentration was measured by scrubberless dual beam UV spectrometry and a Teflon filter and holder (Apex Instruments) was equipped upstream of the inlet as we found the presence of high particle concentration, especially in on-road conditions, produces biased data due to particle penetration into the gas chamber. NO and NO_2 concentrations were measured by single channel chemiluminescence method and the analyser was set with a cycle of 4s for NO and 4s for NO_x as instructed by the manufacturer for high resolution NO_x measurement.

Additionally, a high resolution Global Positioning System (GPS) was used to collect vehicle location data and speed. A camera was installed in the front window to record the on-road conditions for quality assurance while post-processing the plume chasing data, for example confirmation of on-road traffic conditions and individual emission events etc. The information on registration plate numbers of chased vehicles was recorded in the software used for chasing and voice recording was taken for quality control in case of typing error. Each day after the field operation, flow checks were performed for all the particle instruments. The gas analysers were

Table 1
The equipment of OPCAS for plume chasing measurements.

Measurement parameter	Model and manufacturer	Description	Time resolution
CO_2	Carbocap GMP343, Vaisala Inc.	Non-dispersive infrared detector	2s
NO, NO_2, NO_x	CLD66, Eco Physics AG	Chemiluminescence	4s
O_3	211, 2B Technologies	Scrubberless dual beam UV spectrometry	2s
UFP number	CPC 3007, TSI	Condensational particle (d_p > 10 nm) counter for UFP number concentration	1s
$PM_{2.5}$ mass	DustTrak™ II Aerosol Monitor 8530, TSI	Light-scattering laser photometer	1s
Black carbon	AE33, Magee Scientific	Black carbon measurement by light absorption	1s
Temperature and humidity	Q-Trak 7575, TSI	The meteorological measurement concurrently with sampling	1s
Location and speed	BU-353S4 GlobalSat Worldcom Group	USB GPS receiver	1s

calibrated with standard gas every week to confirm data consistency.

Since all the equipment was operated at a high time resolution of seconds (1s–10s), a Matlab script was developed for data acquisition via RS232 communication protocols and a Java script was developed for real time concentration plots display. Simultaneous data collection from all the measuring devices avoids misalignment of data by different time tag among instruments and data synchronization was further performed by aligning the peaks of the measurements obtained.

2.2. Plume chasing measurement

Urban traffic and congestion was avoided by sampling plumes along the main expressways in Hong Kong including the highways from Tsing Yi Island to Lantau Island (Route No. 8), the New Territories Circular Road (Route No. 9) including the Tolo Highway and Fanling Highway as well as Cheung Tsing and Tsing Long Highways (Route No. 3) as shown in Fig. 1. The selection of these highways aimed to cover a variety of vehicle fleets that represent the different functions of the highways, for example, high traffic flow of heavy duty trucks is present on Route 3 and 9 travelling to and from mainland China, while Routes 8 and 9 include many diesel buses. The measurement routes have similar gradients except the western part of route 9 close to Tuen Mun with portion of sloping sections and chasing data collected in this section was excluded from calculations.

The field study took place for 22 sampling days between September 17, 2013 and April 28, 2014. All the measurements were conducted on weekdays between 0900 h and 1700 h. The routes presented in Fig. 1 were repeated more than 3 times for each measurement day. The sampling days were mostly fine, dry and non-overcast. The average monthly temperature and relative humidity were in the range of 21–28 °C, and 43%–65%, respectively. The plume chasing protocol consistently followed previously described methods (Ning et al., 2012; Westerdahl et al., 2009; Wang et al., 2012), in which the mobile platform was driven on relatively empty lanes with stable background concentrations before being positioned inside the plume behind the target vehicle. Next, a distinct vehicle type was targeted and its plume was chased with the mobile platform until a clear CO_2 plume was obtained and the measured pollutant concentrations reached their peak and lasted for at least 30 s according to the real-time data acquisition system. More than 98% of the delta CO_2 concentration between peak and baseline was above 30 ppm with distinct peaks. Usually each vehicle plume was sampled for about two minutes in total

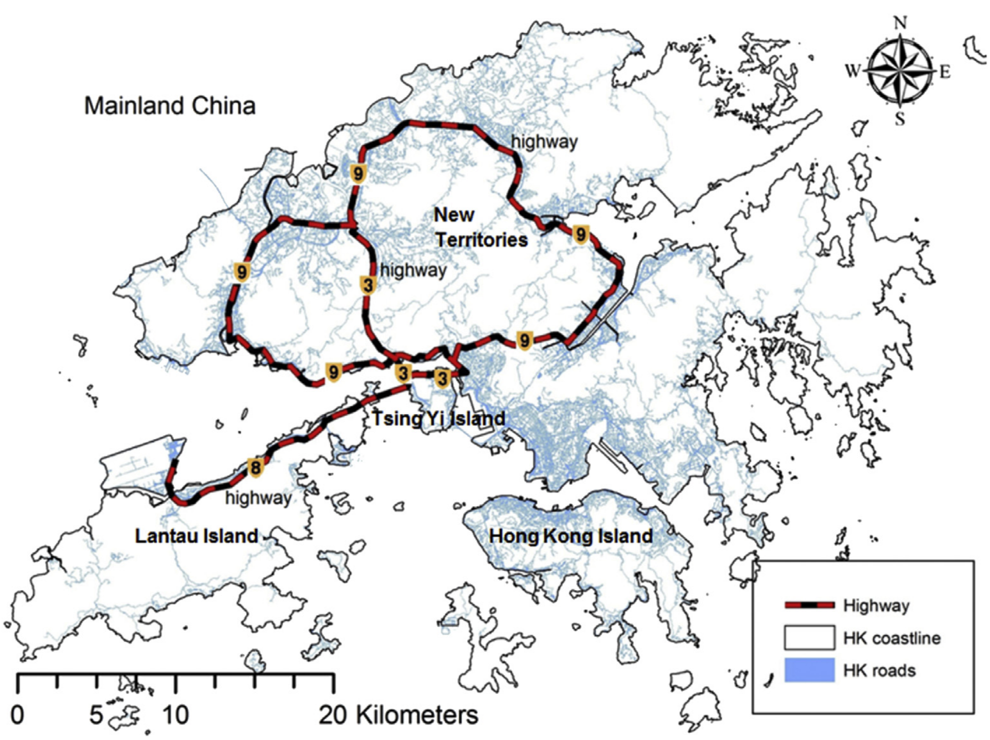

Fig. 1. The map of chasing routes in Hong Kong.

before reliable data could be collected. During the chasing process, the distance between mobile platform and targeted vehicle was maintained at relatively constant value for a stable dilution of the plume (Morawska et al., 2007). Meanwhile, the vehicle license plate number was recorded to retrieve information about its registration for subsequent analysis.

2.3. Data analysis

2.3.1. Emission factor determination

Data analysis and data quality assurance and control procedures followed our previous work as described in Ning et al. (2012). In summary, the time series data for the measured pollutants concentrations were first synchronised to account for the difference in instrument delay time and residence time in the tubing. Individual plume chasing events were identified from a recorded log and video inspection. A Matlab GUI script was developed to load the pollutant concentration data in real time to identify the plume peak and baseline. A certain time window with fixed duration was assigned to the identified peaks and baselines to calculate their individual average concentrations. A sensitivity analysis showed there was no significant difference in the choice of time window of 15 s or 25 s for the peak and baseline (3% difference for BC and 2% difference for NO_x). In the following emission factor calculations, a time window of 15s was used throughout the analysis for consistency.

The emission factors based to the mass of fuel (*EFm)* are defined as the mass of pollutant emitted per mass of fuel consumed (Miguel et al., 1998), and the following equations were used with the assumption that the carbon mass in the vehicle exhaust is mostly in the form of CO_2, with negligible contribution from CO and other carbonaceous compounds (Dallmann et al., 2012; Ning et al., 2012):

$$EFm_p = w_c\left(c_{\mathrm{pl,p}} - c_{\mathrm{bk,p}}\right)\Big/\left(c_{\mathrm{pl,CO_2}} - c_{\mathrm{bk,CO_2}}\right) \tag{1}$$

$$EFm_{p\prime} = 10^{12} w_c\left(c_{\mathrm{pl,p\prime}} - c_{\mathrm{bk,p\prime}}\right)\Big/\left(c_{\mathrm{pl,CO_2}} - c_{\mathrm{bk,CO_2}}\right) \tag{2}$$

where, c is the concentration of pollutant (μg m^{-3}) in the plume (subscript pl) and background (subscript bk) for the pollutants (subscript p), PM, BC and gaseous pollutants in Equation (1), or particles (subscript p′) as particle number cm^{-3} in Equation (2); $c_{\mathrm{pl,CO_2}}$ and $c_{\mathrm{bk,CO_2}}$ represent the concentration of carbon dioxide (mg C m^{-3}) in the plume and background air; w_c is carbon mass fraction. EFm_p is corresponding fuel based emission factor. The plume and background concentration of the pollutants and CO_2 were calculated from the measured data (Wang et al., 2012; Ning et al., 2012) and the w_c value has been reported as 0.87 for diesel (Geller et al., 2005; Dallmann et al., 2012) and this has been used in our work for all vehicles.

2.3.2. Vehicle classification

Each day after plume chasing, the license plate numbers of the observed vehicles were tabulated and sent to the HKEPD to retrieve registration information, which included the manufacture year, license class and engine type. The license class and engine type information was used to assign the vehicles to categories. Diesel goods vehicles in Hong Kong are classified by the permitted gross vehicle weight (GVW) for registration purposes, such that light goods vehicles (LGVs), medium goods vehicles (MGVs) and heavy goods vehicles (HGVs) are defined by GVW $\le$ 5.5 t, 5.5 t < GVW $\le$ 24 t, and GVW > 24 t, respectively, where t represents the metric tonne. As vehicles are commonly classified as heavy duty vehicles where GVW >3.5 t, throughout this study, the combined categories of HGV and MGV were categorised as heavy duty goods vehicles (HDVs). Additionally the study examined plumes from typically large double-decker buses, which in Hong Kong are called franchised buses (FBs) distinguishing them from small sixteen seater public light buses which use liquid petroleum gas (LPG) as a fuel. The manufacture year was used to assign the likely Euro emission standard of the vehicles according to the year of the standard implemented in Hong Kong (summarised in Table S2). There are retrofits such as diesel oxidation catalyst (DOC) and diesel particulate filter (DPF) installed for pre-Euro IV heavy duty diesel vehicles that would reduce their emissions to newer emission standards. However, the current study would not further categorise the vehicles by their retrofitting technology within the classes due to the unavailability of the information from registration database.

2.3.3. Pollutant emission Gini coefficient calculation

The uneven emission contribution made by individual vehicles in a fleet has been well studied and shows that a small fraction of high or super-emitters can contribute a large fraction of total emissions. Variation in vehicle emissions has traditionally been described using standard deviation and skewness (Dallmann et al., 2012). However, here we introduce the vehicle emission Lorenz curve to quantify such a disproportional contribution and the corresponding Gini coefficients are used to represent the significance of high-emitters in total emission control. Mathematically the Gini coefficient is defined by a Lorenz curve, a plot of cumulative income versus cumulative share of people from lowest to highest incomes (Lorenz, 1905), that has been commonly used in economics to represent income distribution. The Gini coefficient is defined as the ratio of the area between the line of equality and Lorenz curve to the area under the line of equality as a measure of inequality of income (an example is depicted in Figure S1). The Gini coefficient varies from 0 to 1, with a higher value for lower equality. In this study, the Lorenz curve was used to describe the distribution of vehicle emission and the derived Gini coefficient was used to quantify the inequality of emission within the fleets. Gini coefficients and their standard error were calculated adopting the algorithm developed by Ogwang (2000) and a Scilab script is shown in Supplementary Information (Appendix A).

2.3.4. Primary NO_2 and NO_x ratio

In this study, NO and NO_x were measured alternatively using one-chamber chemiluminescence apparatus (CLD66, Eco Physics AG). An issue was encountered during this study due to an undocumented instrument built-in data acquisition algorithm; when the measured NO concentration is higher than NO_x recorded in the previous moment, the instrument stops the NO measurement and switches to NO_x detection automatically. This happens occasionally during the plume peak measurements with rapid rising of NO and NO_x concentrations (further detail on this can be found in Figure S2). With the same logic, when the measured NO_x concentration is lower than NO in the previous moment, the NO_x detection stops and switches to NO measurement. Consequently, there were occasions that the NO measurements in the plume were interrupted resulting in an underestimation of NO concentration. Throughout the analysis of NO_2/NO_x ratio, data with such discrepancies were screened out and the ratios were calculated for the validated measurements second by second using the equation:

$$NO_2/NO_x\ ratio = \left(c_{\mathrm{i,NO_2}} - c_{\mathrm{bk,NO_2}}\right)/\left(c_{\mathrm{i,NO_x}} - c_{\mathrm{bk,NO_x}}\right) \tag{3}$$

where $c_{\mathrm{i,NO2}}$ and $c_{\mathrm{i,NOx}}$ are the mixing ratios of pollutants in ppbv at the ith second and $c_{\mathrm{bk,NO2}}$ and $c_{\mathrm{bk,NOx}}$ are the background mixing ratios in ppbv determined by the 5th-percentile mixing ratio 100 s before and after the ith second. The reported NO_2/NO_x ratios were determined by averaging NO_2/NO_x data over 8 s within the plume and excluding the long shut-down period. Finally, successful NO_2/NO_x ratios were recorded for 141 out of 761 diesel vehicles that were chased during the 22-day chasing campaign. With the limitation of this instrument, the sample size for NO_2 and NO_x ratio calculation is smaller.

When NO is emitted from the tailpipe, it reacts with ambient O_3 to form NO_2 and the reverse process also occurs in the presence of sunlight. The inter-conversion of O_3, NO and NO_2 can be summarised in the following reactions:

$$NO + O_3 \rightarrow NO_2 + O_2, \tag{4}$$

$$NO_2 + h\upsilon \rightarrow NO + O, \tag{5}$$

$$O + O_2(+M) \rightarrow O_3(+M) \tag{6}$$

The rate coefficient for reaction (4) is 0.44 $ppm^{-1}\ s^{-1}$ (Atkinson et al., 2004) and the rate of NO_2 photolysis is $5.0 \times 10^{-3}\ s^{-1}$ for half sun (Dickerson and Stedman, 1980). When NO concentration is at around 1 ppm, the time constant for O_3 consumption is around 2 s, while the time constant for NO_2 photolysis is in the order of a hundred seconds. The plume chasing approach measures the NO and NO_2 concentrations 10–20 m from the tailpipe (Ning et al., 2012) and the measured concentrations will likely be affected by ambient O_3 as described in reaction (4), while photolysis of NO_2 is negligible. The investigation of the primary NO_2/NO_x ratio was carried out considering the impact of ozone as in the following sections.

3. Results and discussions

3.1. Overview of vehicles emission factors

Valid on-road data was recorded for a total of 761 diesel vehicles and used for analysis in this study. The sample consisted of 136 (17.9%), 79 (10.4%) and 546 (71.7%) franchised buses, heavy goods vehicles, and medium goods vehicles respectively. Their corresponding average speeds are 67 ± 12 km h^{-1}, 64 ± 13 km h^{-1} and 69 ± 12 km h^{-1}, which were typical driving speeds on Hong Kong highways. The composition of heavy duty goods vehicle fleet (HDVs), combining MGVs and HGVs, according to Euro class showed no significant difference compared to the Hong Kong fleet inventory (χ^2 goodness-of-fit test, $p = 0.07$; further details available from Figure S3), demonstrating the representativeness of the samples from this study for local fleets. The fuel based emission factors (mean ± 95% C.I.) of various pollutants obtained from the different vehicle fleets are summarised in Table 2. Comparing the FBs with HDVs, NO_x emission factors of FBs were significantly higher than HDVs, and vice versa for particle (BC, $PM_{2.5}$ and UFP number) emission factors. The mean NO_x and BC emission factors are within the range of that collected in early 2012 (Ning et al., 2012), with an obvious increase in BC emission factors from HDVs by 37.5% for arithmetic mean, but this increase was not statistically significant, due to the large variation that existed in measured fleet emission factors. The profile of vehicle numbers by Euro class at the

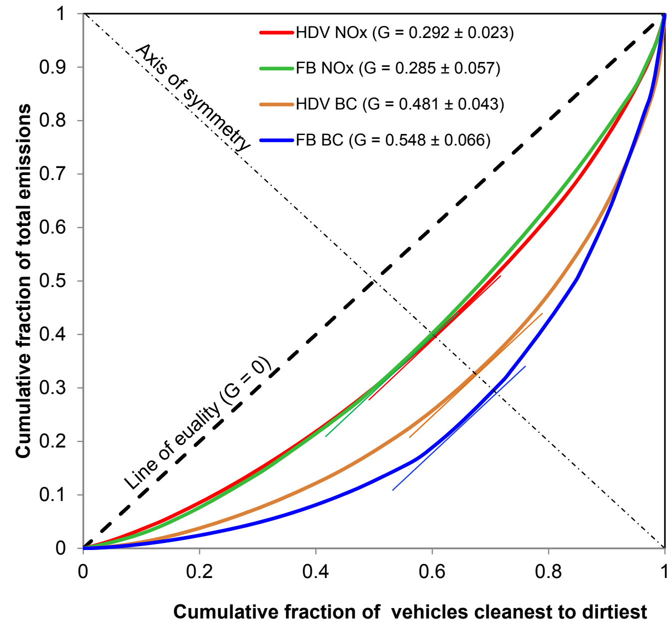

Fig. 2. Lorenz curves for NO_x and BC emissions of different fleets. Numbers in the parentheses are Gini coefficient ± standard error.

end of 2011 and in November 2013, evaluated from the Hong Kong inventory, show significant differences (χ^2 goodness-of-fit test, $p < 0.05$) for both FBs and HDVs. The percentage of Euro IV and V increased by more than 10% for both fleets (Table S3), but no significant decrease was observed in the overall NO_x and BC emission factors. The previous study in 2012 represented a much smaller fleet and no registration information was available, making it difficult for direct comparison of the emission reduction in subsequent Euro classes. It is also worth noting that the replacement of vehicles conforming to newer emission standards doesn't seem to lead to a direct and proportional emission reduction, possibly because replacement might not identify and phase out high or super-emitters. Furthermore, the increased emissions from deterioration of existing fleets may have over-weighted the emission reduction expected through the introduction of newer vehicles.

3.2. Gini coefficients of fleet emissions

Fig. 2 displays the Lorenz curves for NO_x and BC emissions of FBs and HDVs, which are the plots of cumulative fraction of summed emission factors against the cumulative fraction of vehicles counted from the cleanest vehicles. When evaluating the vertical axis from the right hand side in Fig. 2, 15% and 18% of the dirtiest vehicles contributed 50% of the total emission of BC for FBs and HDVs, respectively, while NO_x emissions are slightly more even with about 30% highest emitters contributing to half the total emission. By plotting the tangential line of the Lorenz curves parallel to the line of equality, one could also identify if the Lorenz curve shows symmetry by determining the relative position of tangential point and the axis of symmetry (Damgaard and Weiner, 2000). As shown

Table 2
Fleet-average (±95% CI) emission factors of various pollutants for different fleets.

Vehicle type	Sample size	BC (g/kg-fuel)	$PM_{2.5}$ (g/kg-fuel)	UFP number ($\times 10^{15}$#/kg-fuel)	NO_x (g/kg-fuel)
Franchised bus (FB)	136	1.0 ± 0.2	0.5 ± 0.1	1.2 ± 0.3	39.7 ± 3.9
Heavy duty goods vehicle (HDV)	625	2.2 ± 0.3	1.0 ± 0.1	2.9 ± 0.4	32.3 ± 1.6

in Fig. 2, the NO_x and BC emissions of HDVs yield a symmetric Lorenz curve which suggests their similarity to the lognormal distribution (Damgaard and Weiner, 2000) while BC emission factors of FBs were asymmetrical in the Lorenz curve with longer initial section in the curve meaning relatively larger number of cleaner vehicles in terms of BC emissions in the fleet. This seems to be driven by the active replacement of the Pre-Euro FBs by Euro IV and V categories (details available in Table S3), suggesting more effectiveness in the PM emissions control than the NOx among the local fleets.

Fig. 2 also summarises the results of Gini coefficients for the individual fleet and pollutant. The Gini coefficients for both BC and NO_x emissions suggest no significant difference between HDVs and FBs. On the other hand, both HDVs and FBs have significantly larger Gini coefficients for BC (0.481 and 0.548) emission factors than for NO_x (0.292 and 0.285). Since the Lorenz curves of HDVs are symmetric, large Gini coefficients are attributed to the larger number of vehicles in both extreme ranges of BC emissions (i.e., low and high emission factors). There is also no significant difference in the Gini coefficient for BC emission among various Euro classes (see Table S4 for further detail) and the wide spread of BC emission factors from individual vehicle classes is independent of the Euro standard. Vehicles may have achieved a reduction in BC emissions by applying diesel particulate filter (DPF), but high BC emissions occur when the devices are worn out or poorly maintained. This creates a large difference in overall BC emissions within the fleet as well as within specific Euro classes. Meanwhile, the small Gini coefficient for NO_x emission reflects the difficulty in reducing overall NO_x emissions through the inspection of high-emitters of NO_x.

3.3. Overlapping of high-emitters for different pollutants

Table 3 summarises the degree of overlap among high-emitters of various pollutants. The numbers represent the percentage of vehicles that are common to the top 10% high-emitters of vehicles for the pair of two pollutants. A score of 0 means no overlap, while a score of 100 indicates complete commonality among the dirtiest 10% of the diesel vehicles. In general, high-emitters of BC and $PM_{2.5}$ show high correspondence. In contrast, the degree of overlap between high-emitters of BC and of NO_x is low (<15%). In addition, the dirtiest 10% of BC emitters almost have no or little overlap with the dirtiest 10% of UFP emitters (FBs = 0; HDVs = 13%), clearly demonstrating that high-emitters for one pollutant may not be the same for other pollutants.

Various emission control measures have been applied to different vehicle fleets over the last decade, including the mandatory retrofit of diesel particulate filters (DPF) to the Euro II/III FBs in 2008 (details can be found in Table S1). However, the effectiveness of the control measures has not been systematically evaluated. The top 10% of high $PM_{2.5}$ emitters from FB fleets shows no overlap with high NO_x emitters suggesting the need of coordinated emission control policy, which targets both high-emitters of PM and NO_x. A similar observation was found in on-road vehicle emission studies from different cities (Huo et al., 2012; Wang et al., 2012), which show a lag in NO_x emission reductions with more stringent emission standards compared to PM emissions.

On the other hand, there is also little overlap between PM mass based emission ($PM_{2.5}$ and BC) and PM number emission. Herner et al. (2011) characterised the PM emissions with DPFs and found several orders of magnitude reduction of PM mass accompanied by the nucleation of volatile species formed from sulphate nuclei instead of a soot core. The removal of PM mass emissions reduces total surface areas and facilitates the nucleation of semi-volatile species from exhaust and their ultimate condensation onto the nuclei generating a significant number of ultrafine particles (Ning and Sioutas, 2010). The plume chasing adopted in this study measures the pollutant concentrations inside the plume within 15–20 m of the point of emission from the tailpipe, so the dynamic processes involved may be more complicated than inside the tailpipe as in chassis dynamometer measurement. Both experimental and theoretical investigations of exhaust plumes have shown a rapid growth of nucleation mode particles over short distances; <1 m immediately behind the tailpipe (Uhrner et al., 2007; Wehner et al., 2009). However, few studies examine particle dynamics at the scale of the plume or the roadway (Zhang et al., 2004). The results from our study appear to indicate that nucleation and/or coagulation processes play roles in the intermediate stage from plume to the roadway. Our recent investigation of ultrafine particles and black carbon near a heavily diesel trafficked roadway in street canyon, also showed clear evidence of nucleation from roadway to roadside (Rakowska et al., 2014).

Table 3
Degree of overlap (%) among top 10% high-emitters of various pollutants in FB and HDV fleets.

Fleet	FB (sample size = 87)				HDV (sample size = 393)			
Pollutants	BC	$PM_{2.5}$	UFP	NO_x	BC	$PM_{2.5}$	UFP	NO_x
BC	100				100			
$PM_{2.5}$	69	100			76	100		
UFP	0	11	100		13	18	100	
NO_x	11	0	11	100	13	23	33	100

3.4. Vehicle emissions by Euro classes

A box and whisker plot of NO_x emissions factors for FBs and HDVs by different Euro classes is shown in Fig. 3a. The boxes define the 1st quartile, median, and 3rd quartile with the whiskers extending from the 10^{th}-percentile to the 90th-percentile. The arithmetic mean for each group is plotted as an open square. Boxplots of FB and HDV emission factors both illustrate stepwise reductions in the mean of NO_x emission factors for newer classes of vehicles much as expected. Euro II and III classes for FBs and HDVs show similar interquartile ranges, but FBs have significantly higher EF_{NOx} than HDVs. Bishop et al. (2013) observed that in 1990s, while PM emission reductions were apparent with more stringent standard for heavy duty diesel vehicles, there was also a positive trend for NO_x emissions from the vehicles. This is partly due to a change in the λ value towards higher combustion efficiency, with lower air/fuel ratio at the expense of NO_x emissions. Since the retirement age limit of the diesel vehicles in Hong Kong is 18 years, retrofitting diesel fleets with selective catalytic reduction devices (SCR) and early retirement of older vehicles may be the desired approach to reduce NO_x emissions.

The boxplots in Fig. 3b display the change of BC emission factors with Euro class for FB and HDV fleets. The emission factors for both fleets are shown on the same scale. The median emission factors exhibit a negative trend for both fleets. Pre-Euro class had lower BC emission factors than Euro I for HDVs, which may be the consequence of the mandatory retrofit of diesel oxidation catalyst (DOC) on Pre-Euro HDVs enforced in 2006. Meanwhile, the median BC emission factors for FBs are obviously lower than those for HDVs in Euro II and Euro III class vehicles. These classes of FBs coincidently correspond to buses that were mandatorily retrofitted with DPFs in 2008–2010, while there was no such requirement for the HDV fleet. The decline in emission factors demonstrates that these control measures on particulate reduction were effective for both HDVs and FBs. On the other hand, it is also observed that there is a much larger variation in BC emission factors among the HDV fleets than

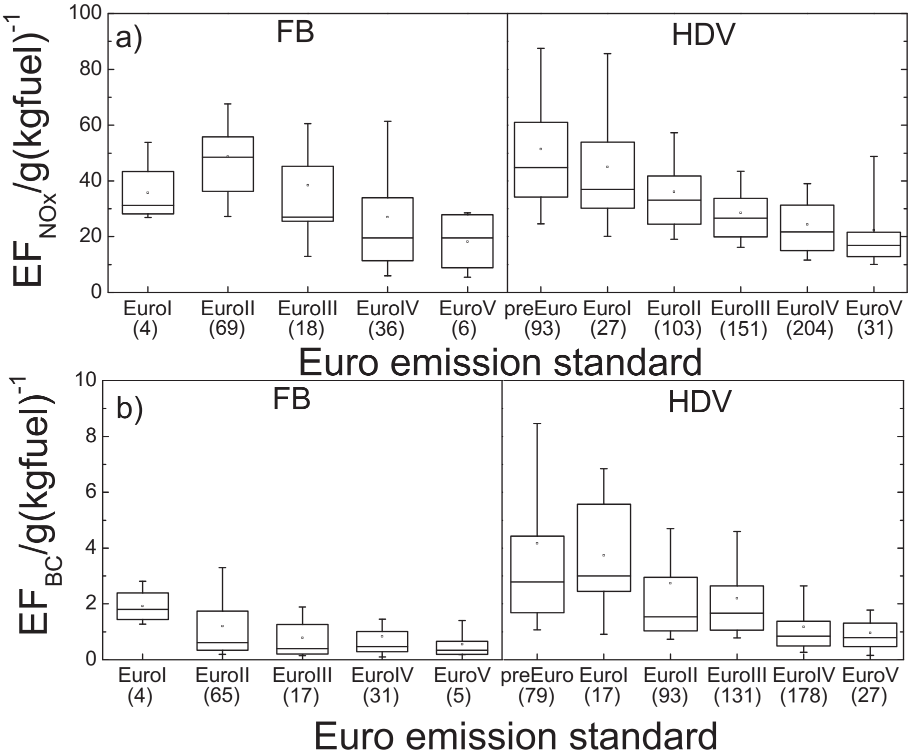

Fig. 3. Boxplots of emissions from different fleets by vehicle design standards. a) NO_x; b) BC. Numbers in the parentheses are vehicle counts by Euro class.

the FB fleets; evidence of the importance of vehicle inspection and maintenance.

The effectiveness of real-world emission reduction with newer standards is evaluated in Fig. 4a which presents the ratios of NO_x emissions factors from FBs and HDVs using Euro II as a reference in comparison with the standard limit values. As the emission standards for heavy-duty diesel engines are on a power rate basis (expressed in g kWh^{-1}), the fuel based emission factors normalised to Euro II from this study can be compared to the standard value under the assumption that fuel efficiency remains constant over time. This is shown by the height of the bar in Fig. 4, while the dotted lines indicate the ratio of emission factor limits assuming a 10% improvement in fuel efficiency from Euro II to Euro V, set as the best possible scenario in fuel efficiency targets. Fig. 4a shows the NO_x emission factor limits relative to Euro II diesel commercial vehicles are 0.7, 0.5 and 0.3 for Euro III, Euro IV and Euro V, respectively. These classes of FBs show good agreement with emission reduction expected from the standard, while HDV NO_x reduction appears to lag behind with much higher ratios for Euro III and newer standards. NO_x emissions from FBs and HDVs were reduced by 55% and 35%, respectively, from Euro II to Euro IV in contrast to the 50% reduction of the standard value.

The Mann–Whitney U tests show that NO_x emission from FBs and HDVs are significantly different based on $p < 0.05$ for both Euro III and Euro IV vehicles. The better performance of FBs may result from the maintenance routines adopted by the franchised operators, compared with a more varied maintenance that is likely to characterise HDVs in private ownership. The SCR technology has been applied in heavy-duty diesel engines to meet the Euro IV and V emission standards. In the SCR system, urea is hydrolysed into ammonia, which reduces NO_x to nitrogen within a specific temperature range in the presence of a catalyst. Bishop et al. (2013) observed that heavy-duty trucks equipped with SCR in the Port of Los Angeles had lower reduction in NO_x emission than expected. It was found that the exhaust pipes temperature may be too low for SCR to perform in cases and low urea levels or malfunction of control devices may result in even higher NO_x emissions.

Fig. 4b displays the performance of real-world FBs and HDVs by comparing the normalised BC emission factors with the standard values of respirable suspended particulates (RSP). Currently there is no BC emission standard and RSP are used here as a surrogate for primary diesel BC emissions since BC has been often used as a tracer for diesel PM emissions as a large proportion is in this form (Chiang et al., 2012; Chin et al., 2012). The mean emission factor for Euro IV was selected as the normalising factor in this case since there was no retrofit for this Euro class. The European emission standard values relative to Euro IV for RSP were tightened sharply from a factor of 7.5 and 5 between Euro II and Euro III for heavy-duty diesel engines. The dotted lines indicate the effect on the ratio of emission factor limits for a possible 10% improvement in fuel efficiency from Euro II to Euro V. Both FBs and HDVs improvements in PM emissions are reflected in Fig. 4b, which shows the normalised BC emissions relative to standard RSP values.

The Mann–Whitney U tests suggest that the normalised BC emission from FBs are significantly lower than that for HDVs for both Euro II ($p = 0.018$) and Euro III ($p = 0.022$) vehicles. Hong Kong adopted ultra-low sulphur diesel (ULSD, 0.005%) in July 2000 so SO_2 emissions from diesel vehicles are low from 2000 onwards. Therefore, one reason for a greater improvement in diesel PM bound BC emissions compared to standard RSP values for Euro II diesel vehicles may arise from a reduction in the sulphur content of fuel. Thus, BC emissions were, in general, reduced further from the standards for both HDVs and FBs. The Hong Kong government has adopted various emission control policies to reduce BC emissions, including (i) mandatory retrofitting of Pre-Euro diesel vehicles with diesel oxidation catalyst (DOC), (ii) retrofitting all Euro II and III

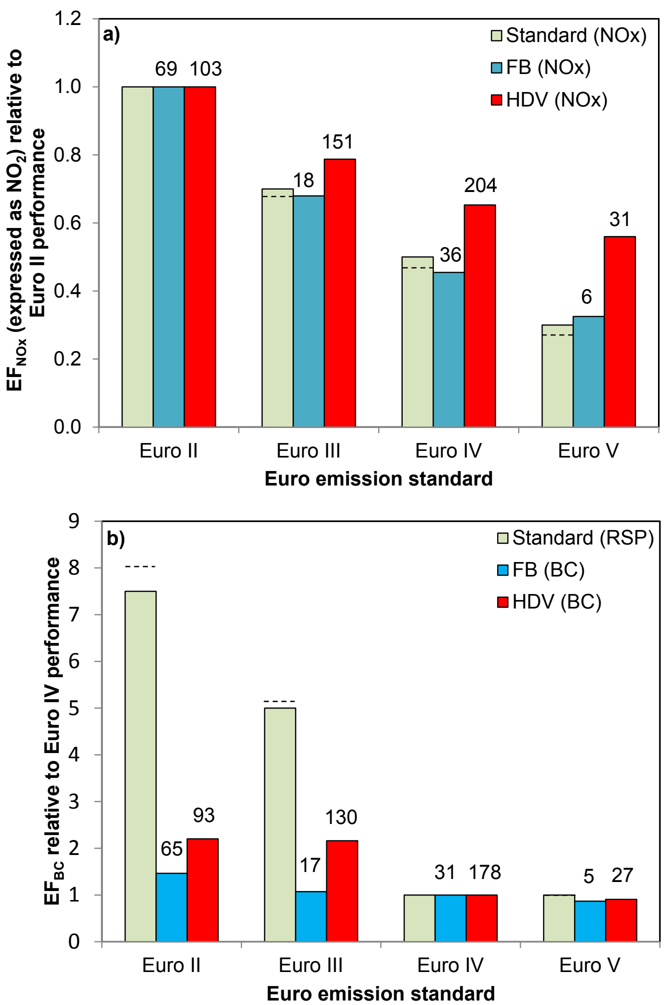

Fig. 4. Comparison of the Euro standard with mean observed emission factors of different fleets (FB and HDV). a) NO_x emission factor b) BC emission factor with RSP surrogate for standard. The numbers on top of the bars are vehicle counts.

franchised buses with DPFs whenever space is available for installation and (iii) implementing fines for smoky vehicles. The results shown in Fig. 4 suggest that the control policies are effective, especially for the older Euro classes, but FBs show a greater reduction of BC emission than HDVs for Euro II and III, as about 90% of FB are fitted with DPF.

Fig. 5 displays Lorenz curve of the contribution of HDVs to the fleet emissions of NO_x and BC by different Euro classes. The ranking of the high emitters in the plots has been arranged with inclusion of all the measured vehicles so the comparison of high emitters among different classes is on the same basis. Fig 5a and b shows the relative emission distribution of the older classes of Pre Euro and Euro I vehicles. A large proportion of these vehicles are found to be in the upper right hand side of the curve for both pollutants with higher contribution to the cumulative emissions, suggesting a larger portion of high emitters in these older classes. Newer vehicles (e.g. Euro IV and Euro V) appear to be distributed more towards the lower left corner of the curve as shown in Fig 5e and f, a clear indication of the overall lower emissions from these newer vehicles, consistent with the emission trend by different Euro classes as shown in Fig. 4. However, it is surprising to see in the distribution that there also exist a considerable number of higher emitters even among the newest Euro IV and V vehicles. The finding raises an interesting question of the cost-effectiveness of emission control by phasing out the old vehicles. For example, if the entire Pre Euro and Euro I HDVs are removed from the on-road fleets, total BC emission would be reduced by 34% according to the distribution results. However, removing the same number of the dirtiest vehicles in the entire HDVs would result in a 52% reduction for BC emissions. Similar results can be also found for NOx emissions with about 9% difference in total emission reduction. The findings highlight the importance of the identification of high emitters on top of the mandatory old vehicles phasing out for cost-effective emission control.

3.5. Primary NO_2/NO_x ratio

The relative abundance of primary NO_2 and background ozone is important in determining primary NO_2 using the plume chasing approach. Single day measurements (from 1000 to 1400 h) were selected to investigate the role of ozone in the primary NO_2 measurements inside the plume. A total of nine vehicles with successful records of NO_2 and NO_x concentrations were studied as shown in Fig. 6. The ambient O_3 from rural background monitoring station (Tap Mun) during the same day showed concentrations in the range of 112–151 ppb, while the on-road O_3 baseline concentration outside plumes was low at 7–38 ppb, resulting from the titration of traffic related NO with high concentrations in the roadway environment. The decrease in O_3 concentrations from the baseline to the inside of the plume was equivalent to the formation of secondary NO_2 in the range of 5–29 ppb. These values are negligible compared to the measured NO_2 concentrations which were typically in the range of 110–786 ppb as shown in Fig. 6. The incremental NO_2 concentration, a result of ozone titration, is less than 10% of the measured NO_2 concentration, demonstrating limited impact of O_3 on the secondary NO_2 formation in the process from tailpipes to the roadway environment. Therefore, the measured NO_2 concentration within the plume can be considered as primary NO_2 in the data analysis. However, it should be noted that the sampling in this study was carried out mostly on heavily trafficked highways, while the ozone concentrations under different roadway conditions may vary depending on the areas of sampling. Rural areas will typically show higher ozone concentrations.

The average primary NO_2/NO_x ratio (p-NO_2/NO_x) from 141 diesel vehicles was found to be 25 ± 14% (average ± one standard deviation). Fig. 7 shows the statistics of p-NO_2/NO_x for different Euro classes. Contrary to the NO_x emission trend, the ratios showed a positive trend for newer Euro classes. In addition, the measured ratios for all Euro classes are well above the typical 5% (by volume) of total NO_x emission for diesel engines. Additionally, there was no reduction in NO_2 emission observed from Euro II onwards in contrast to the great reduction in NO_x emissions. The p-NO_2/NO_x from this study and other studies are summarised in Table 4, with a scattered pattern. Large variations in the NO_2/NO_x emission ratios were commonly reported varying from <10% (by mass) for vehicles without after-treatment (Shorter et al., 2005) to 52% (by volume) for vehicles with after-treatment (Bishop and Stedman, 2008). Kousoulidou et al. (2008) estimated the NO_2/NO_x mass ratio of Euro VI HDVs to be 35% by assuming 45% of the fleet with SCR and DPF, and 55% with exhaust gas recirculation (EGR) and DPF. Carslaw and Rhys-Tyler (2013) also reported that the p-NO_2/NO_x of emissions from buses greatly depends on vehicle manufacturer and the control technology used for Euro IV and V. The NO_2/NO_x ratio by volume was reported to be as low as 0.2% for Euro IV buses equipped with SCR to 19.6% for Euro V buses installed with EGR. Our findings for Euro II and III are quite similar with Carslaw and Rhys-Tyler (2013) and the Euro IV and V are in line with those in Bishop and Stedman (2008) and Kousoulidou et al. (2008) as most of Euro IV

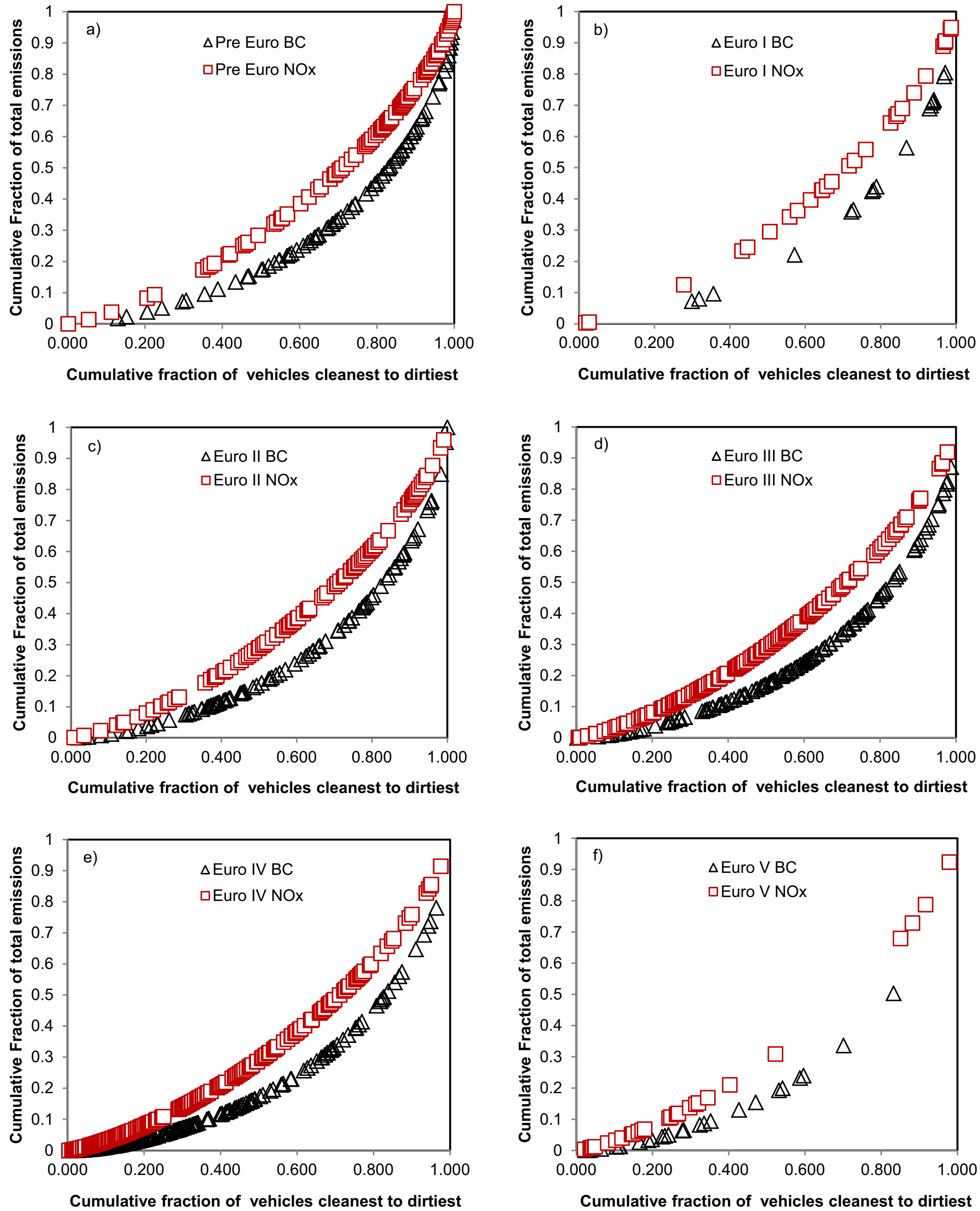

Fig. 5. Cumulative distributions of HDV NO_x and BC emissions for: a) Pre Euro; b) Euro I; c) Euro II; d) Euro III; e) Euro IV and f) Euro V.

and V models in Hong Kong were equipped with EGR systems while SCR were installed mainly on heavy duty vehicles over 10 t (HKEDP, 2006, 2012). The increase in the NO_2/NO_x emissions ratio by Euro classes observed in this study may have a significant effect on recent positive trends in roadside NO_2 concentrations. In many European cities, there have been reports of increases in the urban NO_2/NO_x ratio despite decreasing concentrations of NO_2 (Carslaw, 2005). This trend has also been observed in Hong Kong with *p*-NO_2/NO_x increasing from approximately 2% (by volume) in 1998 to 13% in 2008, and such an increase in NO_2 coincided with the implementation of mandatory retrofit programs for diesel vehicles (Tian et al., 2011). It should be also noted that although this study observed little ozone contribution to the secondary NO_2 formation from tailpipe to the plume, ozone may play a much more significant role in the oxidation of NO as it moves from roadside to the ambient air where it contributes to the overall NO_2 concentrations (Takekawa et al., 2013).

4. Conclusions and implications

The on-road plume chasing measurements made during this work provided a useful approach to quickly collect emission data from a large number of vehicles driven at their on-road conditions. The results show that individual diesel goods vehicles and buses exhibit a wide range of emission factors. The Gini coefficient for fleet emissions represents a quantitative measure of emission disproportionality to prioritize the removal of high-emitters. We have attempted to assess fleet emissions based on the Gini coefficients, so it is clear that high-emitters of different fleets make a disproportionally large contribution to overall traffic emissions. Effective implementation of I/M seems to play an important role in controlling emissions. Different maintenance procedures adopted by franchised bus operators lead to a more skewed distribution of emission factors to lower emissions than that by private HDV operators. However, it is difficult to identify and target these high-

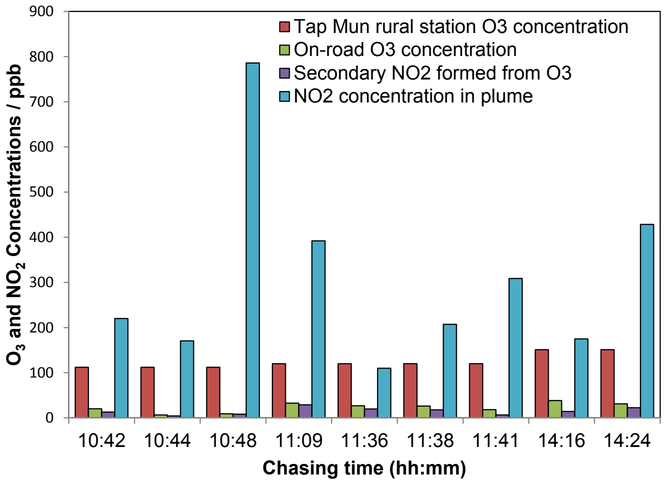

Fig. 6. Concentrations of NO_2 formed from O_3 interaction in contrast to the measured NO_2 concentration in plume.

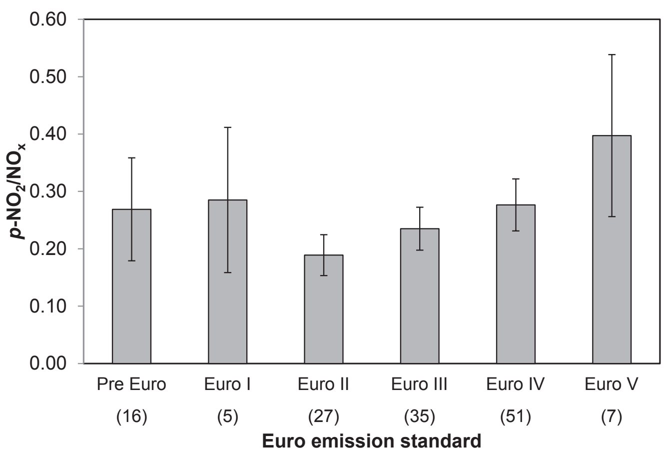

Fig. 7. NO_2/NO_x ratio for combined diesel fleets of FB and HDV by Euro emission class. The numbers in the parentheses are the vehicle counts.

emitters even though Hong Kong has a mandatory annual vehicle examination. Although many cities have deployed the remote sensing systems as a measure of quick screening and identification of high emitters from on-road fleets, the applications have been limited to petroleum and LPG vehicles for gas emission control. Our results clearly demonstrated the urgent need for further technology development and policy implementation of diesel high emitter identification and control, especially for PM emissions. The results from this study indicate that not all the high-emitters are from the older Euro classes. A more cost-effective measure to further improve the urban air quality is to remove dirtiest vehicles rather than replace the oldest vehicles from the diesel fleet. Identification and removal of such high-emitters should be an important component of vehicle emission control strategy.

Meanwhile, there is clear evidence that high-emitters for one pollutant may not be a high-emitter for another pollutant. In particular, there is little overlap among high-emitters in terms of PM mass, PM number and NO_x emissions. Engine technology advances and inappropriate or poorly maintained after-treatment devices (often retrofitted) may pose difficulties in controlling vehicle emissions and lead to poorer roadside and ambient air quality regulators have planned for. This is especially important for the control of particle number emission where ultrafine particles dominate. There are increasing concerns over their potential to create adverse health effects. Although particle number emission has been reduced since the introduction of Euro V and VI classes, little is known on their formation mechanisms and evolution processes beyond the tailpipe. Further investigations are needed to better understand their impact on roadside and ambient air quality in order to reduce the risk of pedestrian exposure in traffic environment.

Lastly, this study has found an increasing, though statistically insignificant, trend of NO_2/NO_x ratios with the introduction of newer emission standards. This appears to support the notion that elevated primary NO_2 emission contributes to the increasing roadside NO_2 concentrations documented in many cities over the last decade. However, a large variation also exists among the same fleet and Euro classes, indicating that the formation mechanism of primary NO_2 emissions may be unstable and depend on driving conditions. On the other hand, after emissions from the tailpipe, the exhaust undergoes dispersion processes in three stages (i) within

Table 4
Summary of NO_2/NO_x ratios for diesel fleets from this study and other sources.

Fleet (literature information)	Method	NO_2/NO_x (mean ± 95% C.I.)	
HDV and FB (present study)	Plume chasing		25 ± 2%
HDV (present study)	Plume chasing	Pre Euro	27 ± 9%
		Euro II	19 ± 4%
		Euro III	24 ± 4%
		Euro IV	28 ± 5%
		Euro V	40 ± 14%
New York, mass transit diesel bus (Shorter et al., 2005)	Chasing	without CRT	<10% (by mass)
		with CRT	33% (by mass)
Sweden, Medium duty diesel bus (Bishop and Stedman, 2008)	On-road remote sensing	Euro III	30%
		DPF EGR	52%
		Euro V	38%
Neverland, HDV (Kousoulidou et al., 2008)	Personal communication from AEAT & TNO 2007	Recommended values	(by mass)
		Euro II and earlier	11%
		Euro III & IV	14%
		Euro V – VI	18%
		Euro VI	35%
UK, Tfl bus (Carslaw and Rhys-Tyler, 2013)	Vehicle emission remote sensing	Euro II (DPF)	19.7 ± 4.6%
		Euro III (DPF)	14 ± 1.6%
		Euro IV (DPF)	15.9 ± 4.1%
		Euro IV (SCR)	0.2 ± 0.2%
		Euro V (EGR)	19.6 ± 3.8%
		Euro V (SCR)	14.4 ± 2.2%

the plume, (ii) from plume to roadside and (iii) from roadside to ambient air. We have also shown by measuring individual vehicle plumes, on heavily trafficked highways, that ozone has a negligible impact on secondary NO_2 formation in the plume. It is expected that in areas with a higher concentration of background ozone, secondary NO_2 formation may have much larger contribution to the both roadside and ambient NO_2 concentrations. Unravelling the relative abundance of primary and secondary NO_2 needs further investigation in order to enact more targeted emission control and air quality policy.

The findings from this study highlight the cost-effectiveness of identification and removal of high emitters from on-road fleets. Multi-pollutant control strategy also needs to be considered in the enactment of the emission control policy which requires more comprehensive retrofitting technological solutions and matching I/M programme to ensure the proper maintenance of fleets.

Acknowledgements

This study was supported by the Environmental Conservation Fund, Hong Kong SAR Government (Ref. No. 01/2012) and the Guy Carpenter Climate Change Centre (Project No. 93610126). The work described herein was also financed in part by the EUROSTARS grant E!4825 FC Aeth and JR-KROP grant 3211-11-000519. The authors would like to thank the Hong Kong Environmental Protection Department (HKEPD) for providing the vehicle registration information and their suggestions on policy implications.

Appendix A. Supplementary data

Supplementary data related to this article can be found at http://dx.doi.org/10.1016/j.atmosenv.2015.09.048.

References

Atkinson, R., Baulch, D.L., Cox, R.A., Crowley, J.N., Hampson, R.F., Hynes, R.G., Jenkin, M.E., Rossi, M.J., Troe, J., 2004. Evaluated kinetic and photochemical data for atmospheric chemistry: volume I – gas phase reactions of O_x, HO_x, NO_x and SO_x species. Atmos. Chem. Phys. 4, 1461–1738.
Attfield, M.D., Schleiff, P.L., Lubin, J.H., Blair, A., Stewart, P.A., Vermeulen, R., Coble, J.B., Silverman, D.T., 2012. The diesel exhaust in miners study: a cohort mortality study with emphasis on lung cancer. J. Natl. Cancer Inst. 104 (11), 869–883.
Baron, P.A., Willeke, K., 2001. Aerosol Measurement - Principles, Techniques, and Applications, second ed. John Wiley & Sons.
Bishop, G.A., Stedman, D.H., 2008. Emissions of Nitrogen Dioxide from Modern Diesel Vehicles. In: WIT Transactions on Ecology and the Environment, vol. 116. WIT Press, pp. 247–254.
Bishop, G.A., Schuchmann, B.G., Stedman, D.H., 2013. Heavy-duty truck emissions in the South Coast Air Basin of California. Environ. Sci. Technol. 47, 9523–9529.
Carslaw, D.C., 2005. Evidence of an increasing NO_2/NO_x emissions ratio from road traffic emissions. Atmos. Environ. 39, 4793–4802.
Carslaw, D.C., Rhys-Tyler, G., 2013. New insights from comprehensive on-road measurements of NO_x, NO_2 and NH_3 from vehicle emission remote sensing in London, UK. Atmos. Environ. 81, 339–347.
Chan, T.L., Ning, Z., Leung, C.W., Cheung, C.S., Hung, W.T., Dong, G., 2004. On-road remote sensing of petrol vehicle emissions measurement and emission factors estimation in Hong Kong. Atmos. Environ. 38, 2055–2066.
Chiang, H.-L., Lai, Y.-M., Chang, S.-Y., 2012. Pollutant constituents of exhaust emitted from light-duty diesel vehicles. Atmos. Environ. 47, 399–406.
Chin, J.-Y., Batterman, S.A., Northrop, W.F., Bohac, S.V., Assanis, D.N., 2012. Gaseous and particulate emissions from diesel engines at idle and under load: comparison of biodiesel blend and ultralow sulfur diesel fuels. Energy Fuels 26, 6737–6748.
Dallmann, T.R., DeMartini, S.J., Kirchstetter, T.W., Herndon, S.C., Onasch, T.B., Wood, E.C., Harley, R.A., 2012. On-road measurement of gas and particle phase pollutant emission factors for individual heavy-duty diesel trucks. Environ. Sci. Technol. 46, 8511–8518.
Damgaard, C., Weiner, J., 2000. Describing inequality in plant size or fecundity. Ecology 81, 1139–1142.
Dickerson, R.R., Stedman, D.H., 1980. Precision of NO_2 photolysis rate measurements. Environ. Sci. Technol. 14, 1261–1262.
Drinovec, L., Močnik, G., Zotter, P., Prévôt, A.S.H., Ruckstuhl, C., Coz, E., Rupakheti, M., Sciare, J., Müller, T., Wiedensohler, A., Hansen, A.D.A., 2015. The "dual-spot" Aethalometer: an improved measurement of aerosol black carbon with real-time loading compensation. Atmos. Meas. Tech. 8, 1965–1979.
Edesess, M., 2011. Roadside air pollution in Hong Kong: why is it still so bad? (Civic Exchange Report).
Franco, V., Kousoulidou, M., Muntean, M., Ntziachristos, L., Hausberger, S., Dilara, P., 2013. Road vehicle emission factors development: a review. Atmos. Environ. 70, 84–97.
Geller, M.D., Sardar, S.B., Phuleria, H., Fine, P.M., Sioutas, C., 2005. Measurements of particle number and mass concentrations and size distributions in a tunnel environment. Environ. Sci. Technol. 39 (22), 8653–8663.
Gertler, A.W., 2005. Diesel vs. gasoline emissions: does PM from diesel or gasoline vehicles dominate in the US? Atmos. Environ. 39, 2349–2355.
Hagler, G., Bergin, M., Salmon, L., Yu, J., Wan, E., Zheng, M., Zeng, L., Kiang, C., Zhang, Y., Lau, A., 2006. Source areas and chemical composition of fine particulate matter in the Pearl River Delta region of China. Atmos. Environ. 40, 3802–3815.
Herner, J.D., Hu, S.H., Robertson, W.H., Huai, T., Chang, M.C.O., Rieger, P., Ayala, A., 2011. Effect of advanced aftertreatment for PM and NO_x reduction on heavy-duty diesel engine ultrafine particle emissions. Environ. Sci. Technol. 45, 2413–2419.
HKEPD, 2006. Euro IV Heavy Duty Vehicle Models. The Hong Kong Environmental Protection Department. http://www.epd.gov.hk/epd/english/environmentinhk/air/guide_ref/files/euroiv_leaflet_eng_1.pdf.
HKEPD, 2011. Primary Nitrogen Dioxide Emissions from Vehicles, CB(1)2291/10–11(01). Administration's paper submitted to Legislative Council Panel on Environmental Affairs. The Hong Kong Environmental Protection Department.
HKEPD, 2012. Euro V Heavy Duty Vehicle Models. The Hong Kong Environmental Protection Department. http://www.epd.gov.hk/epd/english/environmentinhk/air/guide_ref/files/SCR_leaflet_english_2012.pdf.
HKEPD, 2013. Mandatory Retirement of Pre-Euro IV Diesel Commercial Vehicles, CB(1)1820/12–13(01). Administration's paper submitted to Legislative Council Panel on Environmental Affairs. The Hong Kong Environmental Protection Department.
Huo, H., Yao, Z., Zhang, Y., Shen, X., Zhang, Q., He, K., 2012. On-board measurements of emissions from diesel trucks in five cities in China. Atmos. Environ. 54, 159–167.
Kousoulidou, M., Ntziachristos, L., Mellios, G., Samaras, Z., 2008. Road-transport emission projections to 2020 in European urban environments. Atmos. Environ. 42, 7465–7475.
Lorenz, M.O., 1905. Methods of measuring the concentration of wealth. Publ. Am. Stat. Assoc. 9, 209–219.
Louie, P.K.K., Watson, J.G., Chow, J.C., Chen, A., Sin, D.W.M., Lau, A.K.H., 2005. Seasonal characteristics and regional transport of PM 2.5 in Hong Kong. Atmos. Environ. 39, 1695–1710.
Miguel, A.H., Kirchstetter, T.W., Harley, R.A., 1998. On-road emissions of particulate polycyclic aromatic hydrocarbons and black carbon from gasoline and diesel vehicles. Environ. Sci. Technol. 32, 450–455.
Morawska, L., Ristovski, Z.D., Johnson, G.R., Jayaratne, E.R., Mengersen, K., 2007. Novel method for on-road emission factor measurements using a plume capture trailer. Environ. Sci. Technol. 41, 574–579.
Moosmüller, H., Mazzoleni, C., Barber, P.W., Kuhns, H.D., Keislar, R.E., Watson, J.G., 2003. On-road measurement of automotive particle emissions by ultraviolet lidar and transmissometer: instrument. Environ. Sci. Technol. 37, 4971–4978.
Ning, Z., Chan, T.L., 2007. On-road remote sensing of liquefied petroleum gas (LPG) vehicle emissions measurement and emission factors estimation. Atmos. Environ. 41, 9099–9110.
Ning, Z., Sioutas, C., 2010. Atmospheric processes influencing aerosols generated by combustion and the inference of their impact on public exposure: a review. Aerosol Air Qual. Res. 10, 43–58.
Ning, Z., Wubulihairen, M., Yang, F.H., 2012. PM, NO_x and butane emissions from on-road vehicle fleets in Hong Kong and their implications on emission control policy. Atmos. Environ. 61, 265–274.
Ning, Z., Chan, K.L., Wong, K.C., Westerdahl, D., Močnik, G., Zhou, J.H., Cheung, C.S., 2013. Black carbon mass size distributions of diesel exhaust and urban aerosols measured using differential mobility analyzer in tandem with aethalometer. Atmos. Environ. 80, 31–40.
Ogwang, T., 2000. A convenient method of computing the Gini index and its standard error. Oxf. Bull. Econ. Statistics 62, 123–129.
Pakbin, P., Ning, Z., Schauer, J.J., Sioutas, C., 2009. Characterization of particle bound organic carbon from diesel vehicles equipped with advanced emission control technologies. Environ. Sci. Technol. 43, 4679–4686.
Rakowska, A., Wong, K.C., Townsend, T., Chan, K.L., Westerdahl, D., Ng, S., Močnik, G., Drinovec, L., Ning, Z., 2014. Impact of traffic volume and composition on the air quality and pedestrian exposure in urban street canyon. Atmos. Environ. 98, 260–270.
Rubino, L., Bonnel, P., Carriero, M., Krasenbrink, A., 2010. Portable emission measurement system (PEMS) for heavy duty diesel vehicle PM measurement: the European PM PEMS program. SAE Int. J. Engines 2 (2), 660–673.
Schipper, L., Marie-Lilliu, C., Fulton, L., 2002. Diesels in Europe: analysis of characteristics, usage patterns, energy savings and CO_2 emission implications. J. Transp. Econ. Policy 36 (2), 305–340.
Shorter, J.H., Herndon, S., Zahniser, M.S., Nelson, D.D., Wormhoudt, J., Demerjian, K.L., Kolb, C.E., 2005. Real-time measurements of nitrogen oxide emissions from in-use New York city transit buses using a chase vehicle. Environ. Sci. Technol. 39, 7991–8000.

Silverman, D.T., Samanic, C.M., Lubin, J.H., Blair, A.E., Stewart, P.A., Vermeulen, R., Coble, J.B., Rothman, N., Schleiff, P.L., Travis, W.D., Ziegler, R.G., Wacholder, S., Attfield, M.D., 2012. The diesel exhaust in miners study: a nested case–control study of lung cancer and diesel exhaust. J. Natl. Cancer Inst. 104 (11), 855–868.
Takekawa, H., Chatani, S., Ito, A., 2013. A new approach for estimation of the effect of NO_x emission reduction on roadside NO_2 concentration in Tokyo. Atmos. Environ. 68, 92–102.
Tian, L.W., Hossain, S.R., Lin, H.L., Ho, K.F., Lee, S.C., Yu, I.T.S., 2011. Increasing trend of primary NO_2 exhaust emission fraction in Hong Kong. Environ. Geochem. Health 33, 623–630.
Uhrner, U., von Löwis, S., Vehkamäki, H., Wehner, B., Bräsel, S., Hermann, M., Stratmann, F., Kulmala, M., Wiedensohler, A., 2007. Dilution and aerosol dynamics within a diesel car exhaust plume—CFD simulations of on-road measurement conditions. Atmos. Environ. 41, 7440–7461.
Wang, X., Westerdahl, D., Hu, J.N., Wu, Y., Yin, H., Pan, X.C., Zhang, K.M., 2012. On-road diesel vehicle emission factors for nitrogen oxides and black carbon in two Chinese cities. Atmos. Environ. 46, 45–55.
Wehner, B., Uhrner, U., von Löwis, S., Zallinger, M., Wiedensohler, A., 2009. Aerosol number size distributions within the exhaust plume of a diesel and a gasoline passenger car under on-road conditions and determination of emission factors. Atmos. Environ. 43, 1235–1245.
Weiss, M., Bonnel, P., Kühlwein, J., Provenza, A., Lambrecht, U., Alessandrini, S., Carriero, M., Colombo, R., Forni, F., Lanappe, G., 2012. Will Euro 6 reduce the NOx emissions of new diesel cars?–insights from on-road tests with Portable Emissions Measurement Systems (PEMS). Atmos. Environ. 62, 657–665.
Westerdahl, D., Wang, X., Pan, X.C., Zhang, K.M., 2009. Characterization of on-road vehicle emission factors and microenvironmental air quality in Beijing, China. Atmos. Environ. 43, 697–705.
Yang, F., Kaul, D., Wong, K.C., Westerdahl, D., Sun, L., Ho, K.-f., Tian, L., Brimblecombe, P., Ning, Z., 2015. Heterogeneity of passenger exposure to air pollutants in public transport microenvironments. Atmos. Environ. 109, 42–51.
Zhang, K.M., Wexler, A.S., Zhu, Y.F., Hinds, W.C., Sioutas, C., 2004. Evolution of particle number distribution near roadways. Part II: the 'road-to-ambient' process. Atmos. Environ. 38, 6655–6665.